CU-TP-1153
FERMILAB-PUB-06-325-T

The Kaon B-parameter in Mixed Action Chiral Perturbation Theory

C. Aubin,[1,*] Jack Laiho,[2,†] and Ruth S. Van de Water[2,‡]

[1] *Department of Physics, Columbia University, New York, NY 10027*

[2] *Theoretical Physics Department, Fermilab, Batavia, IL 60510*

(Dated: January 19, 2007)

Abstract

We calculate the kaon B-parameter, B_K, in chiral perturbation theory for a partially quenched, mixed action theory with Ginsparg-Wilson valence quarks and staggered sea quarks. We find that the resulting expression is similar to that in the continuum, and in fact has only two additional unknown parameters. At one-loop order, taste-symmetry violations in the staggered sea sector only contribute to flavor-disconnected diagrams by generating an $\mathcal{O}(a^2)$ shift to the masses of taste-singlet sea-sea mesons. Lattice discretization errors also give rise to an analytic term which shifts the tree-level value of B_K by an amount of $\mathcal{O}(a^2)$. This term, however, is not strictly due to taste-breaking, and is therefore also present in the expression for B_K for pure G-W lattice fermions. We also present a numerical study of the mixed B_K expression in order to demonstrate that both discretization errors and finite volume effects are small and under control on the MILC improved staggered lattices.

PACS numbers: 11.15.Ha, 12.39.Fe, 12.38.Gc

*caubin@phys.columbia.edu

†jlaiho@fnal.gov

‡ruthv@fnal.gov

I. INTRODUCTION

Lattice quantum chromodynamics allows nonperturbative calculations of low-energy QCD quantities from first principles. Until recently, limited computing resources and the inability to include quark loop effects have prevented lattice calculations from achieving realistic results. In the past few years, however, lattice simulations of both light meson and heavy-light meson quantities with dynamical staggered quarks have shown excellent numerical agreement with experimental results [1]. These have included both post-dictions, such as the pion and kaon decay constants [2], and predictions, as in the case of the B_c meson mass [3]. Such successes demonstrate that many of the systematic uncertainties associated with lattice simulations are under control, and therefore give confidence that lattice simulations can reliably calculate quantities that cannot be accessed experimentally. One of the simplest quantities of phenomenological importance that can only be calculated using lattice QCD is the kaon B-parameter, B_K. Thus a precise measurement of B_K is an important goal for the lattice community.[1]

B_K parameterizes the hadronic contribution to $K^0-\overline{K}^0$ mixing; it therefore plays a crucial role in extracting information about the CKM matrix using measurements of the neutral kaon system. In particular, the size of indirect CP violation in the neutral kaon system, ϵ_K, when combined with a numerical value for B_K, places an important constraint on the apex of the CKM unitarity triangle [7, 8]. Because ϵ_K is well known experimentally [9], the dominant source of error in this procedure is the uncertainty in the lattice determination of B_K. It is likely that new physics would give rise to CP-violating phases in addition to that of the CKM matrix; such phases would manifest themselves as apparent inconsistencies among different measurements of quantities which should be identical within the standard CKM picture. Thus a precise determination of B_K will help to constrain physics beyond the standard model.

Because lattice simulations with staggered fermions can at present reach significantly lighter quark masses than those with other standard discretizations [10, 11], calculations of weak matrix elements using the available 2+1-flavor Asqtad staggered lattices appear promising. Unfortunately, however, one pays a significant price for the computational speed

[1] Promising calculations of B_K including dynamical quark effects are currently in progress using both improved staggered fermions [4, 5] and domain-wall fermions [6].

of staggered simulations: each flavor of staggered quark comes in four species, or "tastes." In the continuum limit, these species become degenerate and can be removed by taking the fourth root of the fermion determinant. In practice, however, one must take the fourth root of the quark determinant during the lattice simulation in order to remove the extra tastes; thus it is an open theoretical question whether or not one recovers QCD after taking the continuum limit of fourth-rooted lattice simulations. Recently several papers have appeared addressing the validity of the "fourth-root trick" [12, 13, 14, 15, 16]. Although the issue has not yet been resolved, there are indications that the fourth root does not introduce pathologies when taking the continuum limit of the lattice theory. We recommend a recent review by Sharpe, Ref. [17], as a clear summary of the current status of the fourth-root trick. In this paper we assume the validity of the fourth-root trick. Even working under this assumption, however, the additional tastes introduce complications to staggered lattice simulations. The degeneracy among the four tastes is broken by the nonzero lattice spacing, a, and results in discretization errors of $\mathcal{O}(a^2)$. Thus one must use functional forms calculated in staggered chiral perturbation theory (SχPT), in which taste-violating effects are explicit, to correctly extrapolate staggered lattice data [18, 19, 20, 21].

Staggered chiral perturbation theory has been used to successfully fit quantities such as f_π and f_D, for which the SχPT expressions are simple and taste-symmetry breaking primarily enters through additive corrections to the pion masses inside loops [20, 22]. In the case of B_K, however, the additional tastes also make the matching procedure between the lattice $\Delta S = 2$ effective four-fermion operator and the desired continuum operator more difficult. The latticized version of the continuum B_K operator mixes with all other lattice operators that are in the same representation of the staggered lattice symmetry group [23] – including those with different tastes than the valence mesons. Current staggered calculations only account for mixing with operators of the correct taste and only to 1-loop order in α_S; this results in a 20% uncertainty in B_K [4]. In order to achieve a precise determination of B_K with staggered fermions, one must either perform the lattice-to-continuum matching nonperturbatively using a method such as that of the Rome-Southampton group [24] or one must include the effects of the extra operators in the SχPT expression for B_K [25]. Thus far the large number of staggered operators has prevented matching calculations beyond 1-loop order [26, 27], although nonperturbative matching including all relevant staggered operators is, in principle, possible. The effects of this truncated lattice-to-continuum opera-

tor matching can be included in an extended version of SχPT, but the resulting expression for B_K has many undetermined fit parameters, only a few of which are already known from measurements of other quantities. Therefore use of this expression may prove just as difficult as implementing fully nonperturbative matching.

The calculation of weak matrix elements such as B_K with Ginsparg-Wilson (G-W) quarks [28], on the other hand, is theoretically much cleaner than that with staggered quarks. This is because in the massless limit, G-W quarks possess an exact chiral symmetry on the lattice and do not occur in multiple species. Although in practice, lattice simulations use approximate G-W fermions, the degree to which chiral symmetry is broken in simulations can be controlled either by the length of the fifth dimension in the case of domain-wall quarks [29, 30] or through the degree to which the overlap operator is realized in the case of overlap quarks [31, 32, 33]. Consequently, while the $\Delta S = 2$ lattice operator still mixes with wrong-chirality operators, there are significantly fewer operators than in the staggered case, and nonperturbative renormalization can be used in the determination of B_K. As an additional benefit, the approximate chiral symmetry also ensures that the appropriate chiral perturbation theory expression for use in the extrapolation of B_K lattice data is continuum-like at next-to-leading order (NLO). Lattice simulations with G-W fermions, however, are 10 to 100 times more computationally expensive than those with staggered fermions with comparable masses and lattice spacing, and thus are unfortunately not yet practical for realizing light dynamical quark masses.

A computationally affordable compromise is therefore to calculate correlation functions with Ginsparg-Wilson valence quarks on a background of dynamical staggered gauge configurations. This "mixed action" approach combines the advantages of staggered and G-W fermions while not suffering from their major disadvantages, and is well-suited to the calculation of the weak matrix element B_K. By using staggered sea quarks and G-W valence quarks one can better approach the chiral regime in the sea sector while minimizing operator mixing and allowing the use of nonperturbative renormalization. Additionally, because the MILC staggered lattices with 2+1 flavors of dynamical quarks are publicly available and offer a number of quark masses and lattice spacings [10, 11], one can perform unquenched three-flavor simulations at the same cost as quenched G-W simulations. Mixed action simulations have already been successfully used to study quantities of interest to nuclear physics [34, 35], thus we expect that a similar method can be used to calculate B_K.

One might be concerned that the use of a mixed action could introduce new theoretical complications into the lattice determination of B_K. Although the mixed staggered sea, G-W valence lattice theory reduces to QCD in the continuum limit, at nonzero lattice spacing, it is manifestly unphysical in that it violates unitarity. Thus, in order to extract physical QCD quantities from mixed action simulations, it is essential that one can correctly describe and remove contributions due to unphysical mixed action effects from quantities such as B_K using the appropriate lattice chiral perturbation theory. It has not been rigorously proven that the mixed action chiral perturbation theory developed in [36] is the correct chiral effective theory for mixed G-W, staggered simulations in which the fourth-root of the quark determinant is taken in the sea sector. Nevertheless, Ref. [12] showed that, given a few plausible assumptions, staggered chiral perturbation theory is the correct chiral effective theory for describing the pseudo-Goldstone boson sector of rooted staggered simulations. A similar line of reasoning should hold for mixed action chiral perturbation theory. Assuming so, mixed action lattice simulations can be used to correctly calculate quantities involving pseudo-Goldstone bosons (such as B_K) in QCD. More complicated quantities, however, should be considered on a case-by-case basis.

In this paper we calculate B_K in χPT for a lattice theory with G-W valence quarks and staggered sea quarks. We present results for a "1+1+1" theory in which $m_u \neq m_d \neq m_s$ in the sea sector, for a "2+1" theory in which $m_u = m_d \neq m_s$ in the sea sector, and for a "full QCD"-like expression in which we tune the valence-valence meson masses equal to the taste-singlet sea-sea meson masses. (We emphasize, however, that these expressions only truly reduce to QCD when $m_{\rm sea} = m_{\rm valence}$ and the lattice spacing $a \to 0$.) These expressions will be necessary for the correct chiral and continuum extrapolation of mixed-action B_K lattice data. We find that the expression for B_K in mixed action χPT has only two more parameters than in the continuum. The first coefficient multiplies an analytic term which shifts the tree-level value of B_K by an amount of $\mathcal{O}(a^2)$; this term is also present in the case of pure G-W lattice fermions. The second new parameter shifts the mass of the taste-singlet sea-sea meson (which only appears inside loop diagrams) by an amount of $\mathcal{O}(a^2)$. This mass-splitting has already been separately determined, however, in the MILC spectrum calculations so we do not consider it to be an unknown fit parameter. Therefore, in practice, the chiral and continuum extrapolation of mixed action B_K lattice data should be

no more complicated than that of domain-wall lattice data. A numerical analysis using the taste-breaking parameters measured on the MILC coarse lattices ($a \approx 0.125$ fm) shows that the size of non-analytic discretization errors should be less than a percent of the continuum value of B_K over the relevant extrapolation range. In addition, we find that finite volume effects in B_K are also small, and are of $\mathcal{O}(1\%)$ for the lightest pion mass on the MILC coarse ensemble.

This paper is organized as follows. We review mixed action chiral perturbation theory (MAχPT) in Sec. II. In Sec. III we calculate B_K to next-to-leading order in MAχPT. This is divided into four subsections: we first present the spurion analysis necessary to map the quark-level B_K operator onto an operator in the chiral effective theory in Sec. III A, calculate the 1-loop contributions to B_K at NLO in Sec. III B, determine the analytic contributions to B_K at NLO in Sec. III C, and finally present the complete expressions for B_K at NLO in MAχPT in Sec. III D. Next, in Sec. IV, we estimate the numerical size of both taste-symmetry breaking contributions and finite volume effects on the existing MILC ensembles using the resulting mixed action χPT formulae. Finally, we conclude in Sec. V.

II. MIXED ACTION CHIRAL PERTURBATION THEORY

In this section we review the leading-order mixed action chiral Lagrangian, first determined in Ref. [36], and discuss some of its physical consequences for the pseudo-Goldstone boson sector.

We consider a partially quenched theory with N_{val} Ginsparg-Wilson valence quarks and N_{sea} staggered sea quarks. Each staggered sea quark comes in four tastes, and each G-W valence quark has a corresponding bosonic ghost partner to cancel its contribution to loop diagrams. For example, in the case $N_{\text{val}} = 2$ and $N_{\text{sea}} = 3$, the quark mass matrix is given by

$$M = \text{diag}(\underbrace{m_u, m_u, m_u, m_u, m_d, m_d, m_d, m_d, m_s, m_s, m_s, m_s}_{\text{sea}}, \underbrace{m_x, m_y}_{\text{valence}}, \underbrace{m_x, m_y}_{\text{ghost}}), \qquad (1)$$

where we label the dynamical quarks by u, d, and s and the valence quarks by x and y. Near the chiral and continuum limits, the mixed action theory has an approximate $SU(4N_{\text{sea}} + N_{\text{val}}|N_{\text{val}})_L \otimes SU(4N_{\text{sea}} + N_{\text{val}}|N_{\text{val}})_R$ graded chiral symmetry. In analogy with QCD, we

assume that chiral symmetry spontaneously breaks to its vector subgroup,

$$SU(4N_{\rm sea}+N_{\rm val}|N_{\rm val})_L \otimes SU(4N_{\rm sea}+N_{\rm val}|N_{\rm val})_R \xrightarrow{SSB} SU(4N_{\rm sea}+N_{\rm val}|N_{\rm val})_V, \quad (2)$$

and gives rise to $(4N_{\rm sea}+2N_{\rm val})^2-1$ pseudo-Goldstone bosons (PGBs). These PGBs can be packaged in an $SU(4N_{\rm sea}+N_{\rm val}|N_{\rm val})$ matrix:

$$\Sigma = \exp\left(\frac{2i\Phi}{f}\right), \qquad \Phi = \begin{pmatrix} U & \pi^+ & K^+ & Q_{ux} & Q_{uy} & \cdots & \cdots \\ \pi^- & D & K^0 & Q_{dx} & Q_{dy} & \cdots & \cdots \\ K^- & \overline{K}^0 & S & Q_{sx} & Q_{sy} & \cdots & \cdots \\ Q^\dagger_{ux} & Q^\dagger_{dx} & Q^\dagger_{sx} & X & P^+ & R^\dagger_{\widetilde{x}x} & R^\dagger_{\widetilde{y}x} \\ Q^\dagger_{uy} & Q^\dagger_{dy} & Q^\dagger_{sy} & P^- & Y & R^\dagger_{\widetilde{x}y} & R^\dagger_{\widetilde{y}y} \\ \cdots & \cdots & \cdots & R_{\widetilde{x}x} & R_{\widetilde{x}y} & \widetilde{X} & \widetilde{P}^+ \\ \cdots & \cdots & \cdots & R_{\widetilde{y}x} & R_{\widetilde{y}y} & \widetilde{P}^- & \widetilde{Y} \end{pmatrix}, \quad (3)$$

where f is normalized such that $f_\pi \approx 131\,\text{MeV}$. The upper-left block of Φ contains sea-sea PGBs, each of which comes in sixteen tastes. For example,

$$U = \sum_{b=1}^{16} U_b \frac{T_b}{2}\,, \quad (4)$$

where the Euclidean gamma matrices

$$T_b = \{\xi_5, i\xi_\mu\xi_5, i\xi_\mu\xi_\nu, \xi_\mu, \xi_I\} \quad (5)$$

are the generators of the continuum $SU(4)$ taste symmetry (ξ_I is the 4×4 identity matrix). The fields in the central block are the flavor-charged (P^+ and P^-) and flavor-neutral (X and Y) valence-valence PGBs, while those in the lower-right block with tildes are the analogous PGBs composed of only ghost quarks. Finally, the off-diagonal blocks contain "mixed" PGBs: those labelled by R's are composed of one valence and one ghost quark, while those labelled by Q's are composed of one valence and one sea quark. We do not show the mixed ghost-sea PGBs explicitly; their locations are indicated by ellipses.

Under chiral symmetry transformations, Σ transforms as

$$\Sigma \longrightarrow L\,\Sigma\,R^\dagger, \qquad L,R \in SU(4N_{\rm sea}+N_{\rm val}|N_{\rm val})_{L,R}. \quad (6)$$

The standard mixed action chiral perturbation theory power-counting scheme is

$$p^2_{\rm PGB}/\Lambda^2_\chi \sim m_q/\Lambda_{\rm QCD} \sim a^2\Lambda^2_{\rm QCD}\,, \quad (7)$$

so the lowest-order, $\mathcal{O}(p_{\rm PGB}^2, m_q, a^2)$, mixed action chiral Lagrangian is

$$\mathcal{L} = \frac{f^2}{8}\mathrm{Str}\big(\partial_\mu \Sigma\, \partial_\mu \Sigma^\dagger\big) - \frac{\mu f^2}{4}\mathrm{Str}\big(\Sigma M^\dagger + M\Sigma^\dagger\big) + a^2\left(\mathcal{U}_S + \mathcal{U}'_S + \mathcal{U}_V\right), \tag{8}$$

where Str indicates a graded supertrace over both flavor and taste indices and μ is an undetermined dimensionful parameter of $\mathcal{O}(\Lambda_{\rm QCD})$. The leading-order expression for the mass-squared of a valence-valence PGB is identical to that of the continuum because the chiral symmetry of the valence sector prevents an additive shift due to lattice spacing effects:

$$m_{xy}^2 = \mu(m_x + m_y). \tag{9}$$

$\mathcal{U}_S$ and $\mathcal{U}'_S$ comprise the well-known staggered potential and come from taste-symmetry breaking in the sea quark sector [19]. $\mathcal{U}_S$ splits the tree-level masses of the sea-sea PGBs into degenerate groups:

$$m_{ff',t}^2 = \mu(m_f + m_{f'}) + a^2\Delta_t, \tag{10}$$

where Δ_t is different for each of the $SO(4)$-taste irreps: P, V, A, T, I. In particular, $\Delta_P = 0$ because the taste-pseudoscalar sea-sea PGB is a true lattice Goldstone boson. The mixed action Lagrangian contains only one new operator, and thus one new low-energy constant, as compared to the staggered chiral Lagrangian:

$$\mathcal{U}_V = -C_{\rm Mix}\ \mathrm{Str}\big(\tau_3 \Sigma \tau_3 \Sigma^\dagger\big), \tag{11}$$

where

$$\tau_3 = \mathcal{P}_{\rm sea} - \mathcal{P}_{\rm val} = \mathrm{diag}(I_{\rm sea} \otimes I_{\rm taste}, -I_{\rm val}, -I_{\rm val}). \tag{12}$$

This operator links the valence and sea sectors and generates a shift in the mass-squared of a mixed valence-sea PGB:

$$m_{fx}^2 = \mu(m_f + m_x) + a^2\Delta_{\rm Mix}, \qquad \Delta_{\rm Mix} = \frac{16 C_{\rm Mix}}{f^2}\,. \tag{13}$$

Although the parameter $\Delta_{\rm Mix}$ has not yet been calculated in mixed action lattice simulations, it can, in principle, be determined by calculating the mass of a mixed valence-sea meson on the lattice. As in any partially quenched theory, the mixed action theory contains flavor-neutral quark-disconnected hairpin propagators which have double pole contributions. The only flavor-neutral propagators that appear in the expression for B_K are those with two valence quarks; these have the following form:

$$G_{XY}(q) = \frac{\delta_{XY}}{q^2 + m_X^2} + D_{XY}(q), \tag{14}$$

where

$$D_{XY}(q) \;=\; -\frac{1}{3}\frac{1}{(q^2+m_X^2)(q^2+m_Y^2)}\frac{(q^2+m_{U_I}^2)(q^2+m_{D_I}^2)(q^2+m_{S_I}^2)}{(q^2+m_{\pi_I^0}^2)(q^2+m_{\eta_I}^2)} \tag{15}$$

is the disconnected (hairpin) contribution. Note that the sea-sea PGBs in the above expression are all taste singlets because the valence quarks do not transform under the taste symmetry.

III. B_K AT NLO IN MIXED ACTION CHIRAL PERTURBATION THEORY

In this section we outline the calculation of B_K in mixed action χPT. We divide it into four subsections. We first determine the operators that contribute to B_K in the mixed action chiral effective theory using a spurion analysis in Sec. III A. In Sec. III B we outline the 1-loop calculation of B_K, and in Sec. III C we follow this up with an enumeration of the corresponding analytic terms. Finally, the complete NLO results are presented in Sec. III D.

A. B_K Spurion Analysis

The spurion analysis for B_K in the mixed action case is similar to that in the continuum [25, 37]; we will point out differences when they occur.

In continuum QCD, B_K is defined as a ratio of matrix elements:

$$B_K \equiv \frac{\mathcal{M}_K}{\mathcal{M}_{\text{vac}}}\ . \tag{16}$$

The numerator in the above expression measures the hadronic contribution to neutral kaon mixing:

$$\mathcal{M}_K \;=\; \langle \overline{K}^0|\mathcal{O}_K|K^0\rangle, \tag{17}$$

$$\mathcal{O}_K \;=\; [\overline{s}\gamma_\mu(1-\gamma_5)d][\overline{s}\gamma_\mu(1-\gamma_5)d], \tag{18}$$

where we have dropped color indices in $\mathcal{O}_K$ because both color contractions give rise to the same operators in the chiral effective theory. $\mathcal{O}_K$ is an electroweak operator which transforms as a $(27_L, 1_R)$ under the standard continuum chiral symmetry group. The denominator in Eq. (16) is the same matrix element as in the numerator evaluated in the vacuum saturation approximation:

$$\mathcal{M}_K^{\text{vac}} = \frac{8}{3}\langle \overline{K}^0|\overline{s}\gamma_\mu(1-\gamma_5)d|0\rangle\langle 0|\overline{s}\gamma_\mu(1-\gamma_5)d|K^0\rangle, \tag{19}$$

so that B_K is normalized to be of $\mathcal{O}(1)$.

In the mixed action theory, we define B_K in an analogous manner, except that both the external kaons and the operator $\mathcal{O}_K$ must now be composed of valence quarks:

$$\mathcal{O}_K^{\text{lat}} = [\overline{y}\gamma_\mu(1-\gamma_5)x][\overline{y}\gamma_\mu(1-\gamma_5)x]. \tag{20}$$

We can rewrite this operator as follows:

$$\mathcal{O}_K^{\text{lat}} = 4[\overline{q}_L(\gamma_\mu \otimes P_{\overline{y}x})q_L][\overline{q}_L(\gamma_\mu \otimes P_{\overline{y}x})q_L]\,, \tag{21}$$

where the subscript "L" on the quark field indicates the left-handed projection and the matrix $P_{\overline{y}x}$ is a $4N_{\text{sea}} + 2N_{\text{val}}$ matrix in flavor space that projects out the $\overline{y}x$ component of each quark bilinear ($[P_{\overline{y}x}]_{ij} = \delta_{i,14}\delta_{j,13}$ for $N_{\text{sea}} = 3$, $N_{\text{val}} = 2$). If we promote $P_{\overline{y}x}$ to a spurion field, F_K, which can transform under the mixed action chiral symmetry group $SU(4N_{\text{sea}} + N_{\text{val}}|N_{\text{val}})_L \otimes SU(4N_{\text{sea}} + N_{\text{val}}|N_{\text{val}})_R$, then F_K must transform as

$$F_K \to LF_KL^\dagger\,, \tag{22}$$

so that Eq. (21) remains invariant. One cannot build a chirally invariant operator out of Σ and the spurion field F_K without derivatives, but one can build two such operators at $\mathcal{O}(p^2_{\text{PGB}})$:

$$\sum_\mu \text{Str}[\Sigma\partial_\mu\Sigma^\dagger F_K]\text{Str}[\Sigma\partial_\mu\Sigma^\dagger F_K], \tag{23}$$

$$\sum_\mu \text{Str}[\Sigma\partial_\mu\Sigma^\dagger F_K\Sigma\partial_\mu\Sigma^\dagger F_K]. \tag{24}$$

It turns out however, that these two operators are equivalent when one demotes the spurion F_K to the matrix $P_{\overline{y}x}$. Thus we are left with a single chiral operator:

$$\mathcal{O}_K^\chi = \sum_\mu \text{Str}[\Sigma\partial_\mu\Sigma^\dagger P_{\overline{y}x}]\text{Str}[\Sigma\partial_\mu\Sigma^\dagger P_{\overline{y}x}]\,. \tag{25}$$

This operator is identical in form to the continuum B_K operator [37], but Σ contains more fields and the standard trace has been promoted to a supertrace.

Because this operator is of $\mathcal{O}(p^2_{\text{PGB}})$, operators of $\mathcal{O}(m_q)$ and $\mathcal{O}(a^2)$, if present, could also potentially contribute at the same order in χPT. Recall that the quark mass matrix, when promoted to a spurion field, must transform as $M \to LMR^\dagger$; thus we cannot form a chiral operator with a single power of M and two powers of F_K that is invariant under the

chiral symmetry. This is, of course, to be expected because the chiral symmetry of the G-W valence sector and the $U(1)_A$ symmetry of the staggered sea sector are sufficient to prevent any new operators involving the quark mass matrix at leading order in the chiral expansion. New operators of $\mathcal{O}(a^2)$ that are not present in the continuum can also potentially appear and contribute to B_K. As discussed in Ref. [25], such operators arise in two distinct ways: mixing with higher-dimension operators and insertions of four-fermion operators from the action. We demonstrate that these operators do not introduce taste-symmetry breaking, and therefore give rise to the same kinds of analytic terms as in the pure G-W case.

Although the B_K lattice operator is dimension 6, at the level of the Symanzik effective theory, it maps onto all continuum effective operators of dimensions 6 and higher that respect the same lattice symmetries. Operators of dimension 7 and 8 are explicitly suppressed relative to the dimension 6 B_K Symanzik effective operator by powers of a and a^2, respectively, and can therefore be mapped onto chiral operators that may contribute to B_K at NLO. Because, however, the lattice symmetry group includes taste transformations under which the valence quarks are singlets, only dimension 7 and 8 operators composed of four valence quarks can possibly respect the same lattice symmetries as the B_K lattice operator. Moreover, the chiral symmetry of the G-W valence quarks in the B_K operator prohibits strictly valence dimension 7 four-fermion operators. Thus we need only consider dimension 8 Symanzik effective operators for the B_K operator which contain four valence quarks. Fortunately we need not enumerate all possible dimension 8 quark-level operators of $\mathcal{O}(a^2p^2)$ and $\mathcal{O}(a^2m^2)$ in order to determine all possible chiral operators of $\mathcal{O}(a^2p^2_{\mathrm{PGB}})$ and $\mathcal{O}(a^2m_q)$ onto which they map. Because the B_K lattice operator has a L-L chiral structure, and chiral symmetry is respected by the valence sector of the lattice theory, it can only mix with higher-dimension operators that also have a L-L structure. Consequently, these dimension 8 four-fermion operators will generate the same spurions as the dimension 6 B_K operator, and thus lead to the same chiral operator as in Eq. (25), but with an additional undetermined coefficient of $\mathcal{O}(a^2)$. In general, this new coefficient just produces an unknown shift of $\mathcal{O}(a^2)$ to the original $\mathcal{O}(1)$ coefficient of the $\mathcal{O}^\chi_K$. Thus it will not lead to any new functional forms in the expression for B_K in MAχPT, only additional contributions from the leading-order B_K operator that of are higher-order in the MAχPT power-counting. In particular, at NLO in mixed action χPT, it will simply lead to an $\mathcal{O}(a^2)$ correction to the tree-level value of B_K, which we can absorb into an analytic term. We emphasize that, although this contribution

is proportional to a^2, it is not due to taste-symmetry breaking in the staggered sea sector. Because it arises from strictly valence four-fermion operators, it is also present in simulations with pure G-W lattice fermions.

New operators that contribute to B_K at $\mathcal{O}(a^2)$ can also be produced by inserting a dimension 6 $\mathcal{O}(a^2)$ operator from the Symanzik action into the B_K four-fermion operator. A method for combining four-fermion operators at the chiral level was developed in Ref. [21] for the purpose of determining the NLO staggered chiral Lagrangian. This method was later used in Ref. [25] to enumerate the operators that arise from insertions of the staggered action that contribute to B_K with both staggered sea and valence quarks. In the case of the mixed action theory, we must consider insertions of four-fermion operators with only sea quarks, four-fermion operators with only valence quarks, and four-fermion operators with both sea and valence quarks.

Let us first consider insertions of operators with only sea quarks, as all of the work has essentially been done in Ref [25]. Staggered four-fermion operators can be made invariant under arbitrary chiral symmetry transformations by introducing six pairs of spurion fields:

$$\begin{aligned}
&F_L \otimes F_L \to L F_L L^\dagger \otimes L F_L L^\dagger, \qquad && F_R \otimes F_R \to R F_R R^\dagger \otimes R F_R R^\dagger, \\
&F_L \otimes F_R \to L F_L L^\dagger \otimes R F_R R^\dagger, \qquad && \widetilde{F}_L \otimes \widetilde{F}_L \to L \widetilde{F}_L R^\dagger \otimes L \widetilde{F}_L R^\dagger, \\
&\widetilde{F}_R \otimes \widetilde{F}_R \to R \widetilde{F}_R L^\dagger \otimes R \widetilde{F}_R L^\dagger, \qquad && \widetilde{F}_L \otimes \widetilde{F}_R \to L \widetilde{F}_L R^\dagger \otimes R \widetilde{F}_R L^\dagger,
\end{aligned} \tag{26}$$

where the two separate spurions in each pair correspond to the two separate quark bilinears in each four-fermion operator. The taste-breaking spurions in Eq. (26) can be combined with the B_K spurion F_K, which transforms as in Eq. (22), to produce all of the generic chiral structures in Table I.[2] In order to turn these structures into operators that contribute to B_K, one must ultimately replace the spurion fields with constant values. In the case of the staggered theory, because the constituent staggered bilinears may have nontrivial tastes, these spurions become taste matrices, $\xi_i \otimes \xi_i$, which are diagonal in flavor space. In the case of the mixed action theory, because only the staggered sea quarks carry taste quantum numbers, these spurions become taste matrices multiplied by projectors onto the sea sector, i.e. $\xi_i \otimes \xi_i \to \xi_i \mathcal{P}_{\rm sea} \otimes \xi_i \mathcal{P}_{\rm sea}$. For example, consider a particular operator in the mixed action

[2] Note this table is simply the first column of Table III in Ref. [25].

Generic Chiral Structure
$\mathrm{Str}(F_K \Sigma F_R \Sigma^\dagger F_K \Sigma F'_R \Sigma^\dagger) + p.c.$
$\mathrm{Str}(F_K \Sigma F_R \Sigma^\dagger)\mathrm{Str}(F_K \Sigma F_R \Sigma^\dagger) + p.c.$
$\mathrm{Str}(F_K \widetilde{F_L} \Sigma^\dagger F_K \Sigma \widetilde{F_R}) + p.c.$
$\mathrm{Str}(F_K \widetilde{F_L} \Sigma^\dagger)\mathrm{Str}(F_K \Sigma \widetilde{F_R}) + p.c.$
$\mathrm{Str}(F_K \widetilde{F_L} \Sigma^\dagger F_K \widetilde{F_L} \Sigma^\dagger) + p.c.$
$\mathrm{Str}(F_K \widetilde{F_L} \Sigma^\dagger)\mathrm{Str}(F_K \widetilde{F_L} \Sigma^\dagger) + p.c.$

TABLE I: Mesonic operators corresponding to insertions of four-fermion operators from the Symanzik effective action; these generic structures apply to operators with only sea quarks, to those with only valence quarks, and to mixed operators with both sea and valence quarks. F_K comes from the B_K quark-level operator and will ultimately be set equal to the projector $P_{\overline{y}x}$. The remaining spurions come from four-fermion operators, and must be set equal to different matrices depending upon the four-fermion operator under consideration; the specific details are discussed in the text. The notation "p.c." indicates the parity-conjugate of the previous operator.

theory coming from the first spurion combination in Table I:

$$\mathrm{Str}(F_R \Sigma F_K \Sigma^\dagger F_R \Sigma F_K \Sigma^\dagger) + p.c. \xrightarrow{\text{sea-sea f-f. op.}} \mathrm{Str}(\xi_5 \mathcal{P}_{\mathrm{sea}} \Sigma P_{\overline{y}x} \Sigma^\dagger \xi_5 \mathcal{P}_{\mathrm{sea}} \Sigma P_{\overline{y}x} \Sigma^\dagger) + p.c. \quad (27)$$

Because this operator is already of $\mathcal{O}(a^2)$, it can only contribute to B_K at NLO through tree-level diagrams; thus it can only contain two pion fields, which are insufficient to separate all of the projectors onto the sea sector from all of the projectors on the valence sector. In fact, it is easy to show that none of the chiral operators arising from insertions of staggered four-fermion operators actually contribute to B_K at NLO (although they may at higher orders) because their contributions vanish identically due to the fact that $\mathcal{P}_{\mathrm{sea}} P_{\overline{y}x} = 0$. Thus we do not show all of their expressions here.

We next consider insertions of mixed four-fermion operators in which one quark bilinear contains staggered sea quarks and the other contains GW valence quarks. Such mixed operators can be made invariant under arbitrary chiral symmetry transformations with the following four pairs of spurion fields [36]:

$$\begin{aligned} &F_L \otimes F_L \to L F_L L^\dagger \otimes L F_L L^\dagger, \qquad F_R \otimes F_R \to R F_R R^\dagger \otimes R F_R R^\dagger, \\ &F_L \otimes F_R \to L F_L L^\dagger \otimes R F_R R^\dagger, \qquad F_R \otimes F_L \to R F_R R^\dagger \otimes L F_L L^\dagger, \end{aligned} \quad (28)$$

where, in this case, we have distinguished between the first spurion in the pair (which corresponds to the sea bilinear) and the second spurion (which corresponds to the valence bilinear). This is necessary because the sea spurion will ultimately be replaced with a projector onto the sea sector, while the valence spurion will become a projector on the valence sector. By comparing Eqs. (28) and (26), one can see that the mixed spurion fields are actually a subset of the staggered spurion fields, although they must be replaced with different matrices in order to produce operators that contribute to B_K. Consequently, the only possible combinations of the B_K spurion with the mixed spurions are already given in the upper panel of Table I. Although the mixed case is clearly similar to the staggered one, let us nevertheless consider the example of the operator arising from the first generic structure in Table I:

$$\mathrm{Str}(F_R\Sigma F_K\Sigma^\dagger F_R\Sigma F_K\Sigma^\dagger) + p.c. \xrightarrow{\text{sea-val f-f. op.}} \mathrm{Str}(\mathcal{P}_{\text{sea}}\Sigma P_{\overline{y}x}\Sigma^\dagger\mathcal{P}_{\text{val}}\Sigma P_{\overline{y}x}\Sigma^\dagger) + p.c. \qquad (29)$$

This operator does not contribute to B_K at NLO for the same reasons as the previous example, and neither does the other operator arising from insertions of mixed valence-sea four-fermion operators.

Finally, we consider insertions of purely valence four-fermion operators. These operators lead to the same spurion fields as the mixed operators [36], and thus to the same chiral forms in the upper panel of Table I. The only difference is that both spurion fields must be replaced with projectors onto the valence sector. Consequently, as in the case of the previous example, the new chiral operators do not contribute to B_K at NLO. In summary, although many MAχPT operators of $\mathcal{O}(a^2)$ arise from insertions of four-fermion operators in the Symanzik effective action, none of them contribute to B_K at NLO for the mixed G-W, staggered lattice theory.

The previous analysis holds for G-W valence quarks, which have perfect chiral symmetry. On the lattice however, G-W quarks are often approximated as domain-wall quarks, which have a small amount of residual chiral symmetry breaking due to the finite size of the fifth dimension. This chiral symmetry breaking is parameterized by the residual mass, m_{res}, which is a measure of how far the left- and right-handed components of the quarks extend into the fifth dimension. These effects can be readily added to the chiral theory, as seen in Refs. [38, 39], by adding the following mass-like term to the chiral Lagrangian:

$$\Delta\mathcal{L}^{\text{DWF}} = -\frac{\mu f^2}{4}\mathrm{Str}\big(\Sigma\Omega^\dagger + \Omega\Sigma^\dagger\big), \qquad (30)$$

where Ω is a spurion which transforms as the mass matrix transforms, and in the end we set $\Omega = m_{\rm res} \times I$. This leads to the familiar expression for the tree-level mass of a PGB composed of two domain-wall quarks:

$$m_{xy}^2 = \mu(m_x + m_y + 2m_{\rm res}). \tag{31}$$

Clearly this term will not contribute at leading order to B_K, since the Ω spurion transforms in the same manner as the mass spurion, and the mass term did not contribute at this order. Consequently, one may simply shift the valence quark masses by $m_{\rm val} \to m_{\rm val} + m_{\rm res}$ in the results of this paper to transform them into expressions that apply to lattice simulations with domain-wall valence quarks and staggered sea quarks.[3]

Finally we must consider the fact that, while one constructs a lattice operator to correspond to a continuum operator with a particular spin, once on the lattice, this operator is allowed to mix due to gluon exchange with operators that correspond to other continuum spin structures. This comes from the fact that the symmetry group on the lattice is not the $SO(4)$ group of Euclidean rotations: it has been broken down to the subgroup of hypercubic rotations. Lattice operator mixing patterns can become especially complicated when one introduces staggered quarks because now the desired lattice operator can not only mix with other operators with incorrect spins, but also those with incorrect tastes. Fortunately, in the mixed action theory that we consider here, the symmetry of the G-W valence sector is sufficient to prevent mixing between the lattice B_K operator and new operators with nontrivial taste structure. Because the valence quarks in the B_K four-fermion operator do not transform under taste symmetry, the B_K operator is clearly not in the same lattice symmetry irrep as any taste-violating four-fermion operators. Furthermore, in the case of pure G-W valence quarks, the B_K operator cannot mix with operators of the wrong chirality. In realistic simulations with domain-wall valence quarks, however, the desired lattice B_K operator with spin structure $VV + AA$ mixes with four other operators which do not have the same $VV + AA$ spin structure (TT, $VV - AA$, $SS + PP$, and $SS - PP$). This

[3] In applying χPT expressions to lattice simulations with domain-wall valence quarks and staggered sea quarks, it is also important to remember that the domain-wall valence and staggered sea quark masses are renormalized differently. Consequently, if one wishes to use the bare domain-wall lattice Dirac mass parameter and the bare AsqTad staggered lattice mass in mixed action χPT expressions, one must allow the parameter μ which relates the quark masses to the pion mass-squared to be different in the valence and sea sectors.

contamination though is suppressed by two factors of the residual mass [40], and the effect is small, so long as the residual mass is small. Although the effect may be small, it could be non-negligible, but then it can be removed nonperturbatively using the standard method of Rome-Southampton [24].

To summarize, the result of this spurion analysis is that the leading order operator that contributes to B_K in the mixed action case is simply the continuum operator naively generalized to the mixed action theory. This is simpler than the full staggered case [25], in which many new operators appeared at leading order due to taste-symmetry breaking. Nevertheless, taste-symmetry breaking will still enter the mixed action calculation of B_K through the masses of PGBs in loop diagrams. In addition, taste-breaking operators will generate operators of next-to-leading order (NLO) in the chiral effective theory that will contribute to analytic terms; we will discuss these in Sec. III C.

B. Contribution of B_K at 1-Loop

Recall from Eq (16) that the kaon B-parameter is defined as the ratio $\mathcal{M}_K/\mathcal{M}_K^{\text{vac}}$. At tree-level,

$$\left(\frac{\mathcal{M}_K}{\mathcal{M}_K^{\text{vac}}}\right)^{LO} \equiv B_0. \tag{32}$$

Because all higher-order contributions to B_K are identically zero in the limit of massless quarks, this expression defines the B-parameter in the chiral and continuum limits.

At 1-loop, the $K^0 - \overline{K}^0$ matrix element receives contributions from the diagrams shown in Fig. 1, where we have specified the location of each of the two left-handed currents in the chiral operator $\mathcal{O}_K^{\chi}$.[4] This factorization of the operator is useful because the calculation of the kaon matrix element can then be separated into two pieces, the 1-loop corrections to f_K and the 1-loop corrections to B_K in which we are interested. In terms of the contributions from the diagrams in Figure 1, the B_K matrix element can be written as

$$\mathcal{M}_K = \frac{8}{3} B_0 f^2 m_{xy}^2 \{1 + X[\text{Figs. 1(b)-(c)}]\} + X'[\text{Figs. 1(d)-(f)}]\}, \tag{33}$$

[4] Note that this factorization is only possible at leading order. At higher orders, B_K receives contributions from operators which are not simply products of left-handed currents.

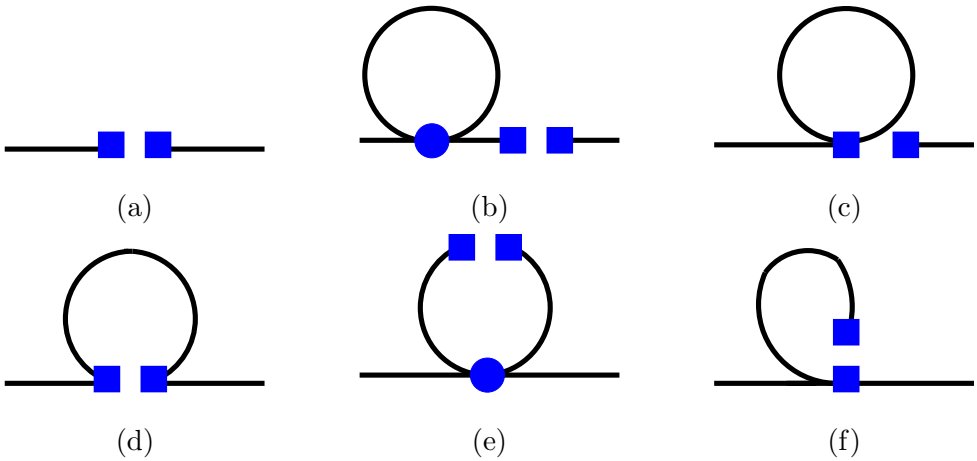

FIG. 1: Tree-level and 1-loop contributions to $\mathcal{M}_K$. The circle represents a vertex from the LO staggered chiral Lagrangian. Each square represents an insertion of one of the two left-handed currents in $\mathcal{O}_K^\chi$ and "changes" the quark flavor from $d \leftrightarrow s$.

where X and X' indicate the results of specific diagrams and m_{xy}^2 is the 1-loop kaon mass squared. At 1-loop, the form of $\mathcal{M}_K^{\text{vac}}$ is simple:

$$\mathcal{M}_K^{\text{vac}} = \frac{8}{3} m_{xy}^2 f_{xy}^2, \tag{34}$$

where m_{xy}^2 and f_{xy} are the 1-loop corrected values. It is clear that diagrams (b) and (c) in Fig. 1 factorize – the left-half of each diagram is the 1-loop correction to f_K, while the right half is just f at tree-level. Mathematically,

$$X[\text{Figs. 1(b)-(c)}] = 2\frac{\delta f_{NLO}}{f}, \tag{35}$$

where the factor of two comes from the fact that the loop can appear on either leg. Diagrams 1(b) and 1(c) therefore turn the leading order f^2 into the 1-loop f_{xy}^2 in Eq. (33):

$$\mathcal{M}_K = \frac{8}{3} B_0 f_{xy}^2 m_{xy}^2 + X'[\text{Figs. 1(d)-(f)}], \tag{36}$$

such that B_K at one loop only depends on diagrams 1(d)-(f):

$$B_K^{1-loop} = B_0 + \frac{3}{8}\frac{X'[\text{Figs. 1(d)-(f)}]}{f_{xy}^2 m_{xy}^2}. \tag{37}$$

Figure 2 shows the quark flow diagrams that correspond to the meson diagrams in Figs. 1(d)-(f). It is interesting to note that the only place where sea quarks appear in these diagrams is in the disconnected hairpin propagators of diagrams 2(b) and (c). In

particular, there are no contributions from mixed mesons made of one sea and one valence quark, so the new parameter in the mixed-action chiral Lagrangian, $\Delta_{\rm Mix}$, does not appear in B_K to 1-loop.[5]

We now proceed to calculate the 1-loop contributions to B_K from Figure 2. The connected diagrams, 2(a), (d), and (e), combine to give the result[6]

$$\mathcal{M}_{conn} = \frac{B_0}{6\pi^2}\int \frac{d^4q}{(2\pi)^4}\left[\frac{2m_{xy}^4}{q^2+m_{xy}^2} - \frac{m_X^2+m_{xy}^2}{q^2+m_X^2} - \frac{m_Y^2+m_{xy}^2}{q^2+m_Y^2}\right]. \tag{38}$$

The contribution from the disconnected diagrams, 2(b) and (c), is somewhat more tedious to evaluate because of the double poles in the hairpin propagators:

$$\mathcal{M}_{disc} = \frac{2}{3}B_0\int \frac{d^4q}{(2\pi)^4}(m_{xy}^2+q^2)\left\{D_{xx}^I(q)+D_{yy}^I(q)-2D_{xy}^I(q)\right\}, \tag{39}$$

where D_{ij}^I is the taste-singlet disconnected propagator of Eq (15). Making use of the identity [25],

$$D_{xx}+D_{yy}-2D_{xy} = (m_X^2-m_Y^2)^2\frac{\partial}{\partial m_X^2}\frac{\partial}{\partial m_Y^2}\{D_{xy}\}, \tag{40}$$

we get the following result for the disconnected piece in the "1+1+1" partially quenched theory:

$$\mathcal{M}_{disc}^{PQ,1+1+1} = \frac{B_0}{48\pi^2}(m_X^2-m_Y^2)^2\frac{\partial}{\partial m_X^2}\frac{\partial}{\partial m_Y^2}\left\{\int\frac{d^4q}{(2\pi)^4}\sum_j\frac{(m_{xy}^2+m_j^2)}{(q^2+m_j^2)}R_j^{[4,3]}(\{M_{XY,I}^{[4]}\};\{\mu_I^{[3]}\})\right\}, \tag{41}$$

where $R_j^{[4,3]}$ is the residue arising from the double pole in the disconnected propagator; $R_j^{[4,3]}$, $\{M_{XY,I}^{[4]}\}$, and $\{\mu_I^{[3]}\}$ are defined in Sec. III D.

To get the full expression for B_K at NLO, one must combine the 1-loop contributions with analytic terms that arise from tree-level matrix elements of higher-order operators:

$$B_K^{PQ} = B_0 + \frac{3}{8}\left(\frac{\mathcal{M}_{conn}+\mathcal{M}_{disc}}{f_{xy}^2 m_{xy}^2} + \text{analytic terms}\right). \tag{42}$$

We discuss the analytic terms in the following subsection.

[5] This cancellation of chiral logarithms containing the parameter $\Delta_{\rm Mix}$ is not unique to B_K. It also occurs in other mixed action chiral perturbation theory expressions when they are written in terms of 1-loop PGB masses and decay constants (rather than bare parameters), such as in the case of the $I=2$ $\pi\pi$ scattering amplitude [41].

[6] We note that, although all of the integrals in this section are divergent in four dimensions, one can choose a suitable regulator to make them finite before their evaluation; this regulator can then be removed after the results have been renormalized.

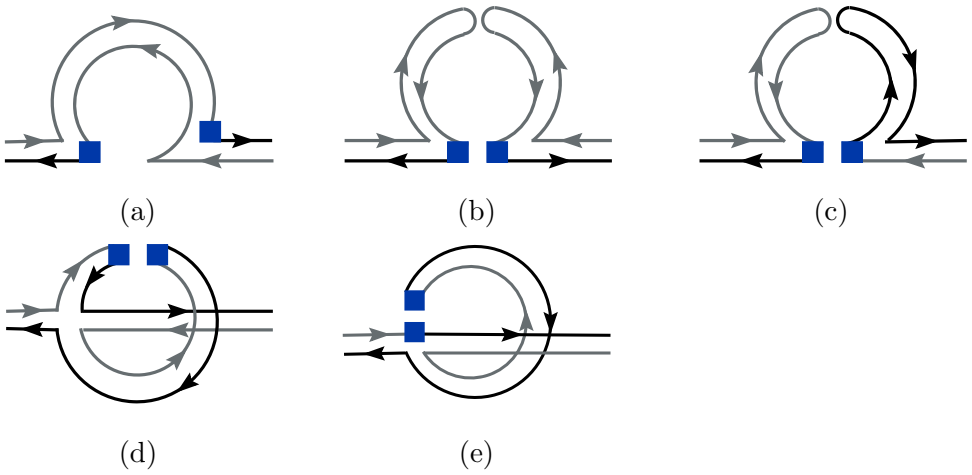

FIG. 2: Quark flow diagram contributions to B_K at 1-loop. One external meson is a $\overline{K}^0$ and the other is a K^0. The two boxes represent an insertion of the B_K operator. Each box "changes" the valence quark flavor from $d \leftrightarrow s$. Diagrams (a)–(c) contribute to Fig. 1(d), diagram (d) contributes to Fig. 1(e), and diagram (e) contributes to Fig. 1(f).

C. Analytic contributions to B_K at NLO

Next-to-leading order analytic contributions to B_K come from tree-level matrix elements of NLO operators. In MAχPT, such terms can come from operators of the following order in the power-counting scheme:

$$\mathcal{O}(p^4_{\rm PGB}),\ \mathcal{O}(a^2 p^2_{\rm PGB}),\ \mathcal{O}(a^4),\ \mathcal{O}(m_q^2),\ \mathcal{O}(p^2_{\rm PGB} m_q),\ \mathcal{O}(a^2 m_q). \tag{43}$$

There are many such operators in the mixed action chiral Lagrangian, however, since it is not necessary to separate them in fits to numerical lattice data, we do not enumerate them all here. Instead we use symmetry arguments to restrict the possible linearly independent terms as in Ref. [25].

First we discuss those analytic contributions which are easiest to determine. One can immediately rule out contributions from operators of $\mathcal{O}(p^4_{\rm PGB})$ because such operators contain four derivatives, but tree-level matrix elements contain only two fields upon which they can act. One can also rule out contributions from $\mathcal{O}(a^4)$ operators because, at tree-level, they would produce terms without powers of masses in them, and the chiral symmetry of the valence sector requires that the kaon matrix element vanishes in the chiral limit. Finally, all contributions from $\mathcal{O}(a^2 p^2_{\rm PGB})$ operators must be proportional to m^2_{xy} because the derivatives must act on the two external kaons, giving a factor of p^2 which becomes m^2_{xy} when the

kaons are on-shell. This leads to the first analytic term: $c_1 a^2 m_{xy}^2$.

All of the analytic terms that are not proportional to powers of a^2 are the same as in the continuum partially quenched theory. The mass dependence of these terms can be determined using CPS symmetry [42], where C and P are the usual charge conjugation and parity reversal symmetries, respectively. In QCD, S corresponds to the exchange of d and s quarks, however, in the mixed action lattice theory, we must impose a symmetry under the interchange of x and y valence quarks instead: $x \leftrightarrow y$, $m_x \leftrightarrow m_y$. There are only two linearly independent $\mathcal{O}(m_q^2)$ terms allowed by this symmetry; we choose to write them in the forms $c_2 m_{xy}^4 \propto c_2(m_x + m_y)^2$ and $c_3(m_x - m_y)^2$. Operators of $\mathcal{O}(p_{\rm PGB}^2 m_q)$ only contribute one new linear combination of masses: $m_{xy}^2 \mathrm{Tr}(M_{\rm sea})$, where $M_{\rm sea}$ is the $N_{\rm sea} \times N_{\rm sea}$ sea quark mass matrix.

Finally, operators of $\mathcal{O}(a^2 m_q)$ can be shown to give no new independent contributions. There are three possibilities for the quark mass dependence: $(m_x + m_y)$, $(m_x - m_y)$, and $\mathrm{Tr}(M_{\rm sea})$. The first term, $a^2(m_x + m_y)$, is already included in c_1, the second, $a^2(m_x - m_y)$, is forbidden by CPS symmetry, while the last term, $a^2 \mathrm{Tr}(M_{\rm sea})$, vanishes for the following reason. The factor $\mathrm{Tr}(M_{\rm sea})$ always comes from the operator $\mathrm{Str}(\Sigma M^\dagger + M\Sigma^\dagger)$ when $\Sigma = 1$, so the only operators that can lead to contributions of the form $a^2 \mathrm{Tr}(M_{\rm sea})$ are $\mathcal{O}(a^2)$ operators multiplying $\mathrm{Str}(\Sigma M^\dagger + M\Sigma^\dagger)$. However, by chiral symmetry, the $\mathcal{O}(a^2)$ operators cannot generate tree-level contributions to $\mathcal{M}_K$. Therefore, the $a^2 \mathrm{Tr}(M_{\rm sea})$ terms also vanish.

To summarize, the following analytic terms contribute to B_K at NLO:

$$\left[c_1 a^2 m_{xy}^2, \quad c_2 m_{xy}^4, \quad c_3(m_X^2 - m_Y^2)^2, \quad c_4 m_{xy}^2 (m_{U_P}^2 + m_{D_P}^2 + m_{S_P}^2)\right]. \tag{44}$$

Note that we have re-expressed them in terms of meson masses, rather than quark masses, because those are what one measures in a lattice simulation.

D. Next-to-Leading Order B_K Results

In this section we present results for a "1+1+1" theory in which $m_u \neq m_d \neq m_s$ in the sea sector, for a "2+1" theory in which $m_u = m_d \neq m_s$ in the sea sector, and for a "full QCD"-like expression in which we tune the valence-valence meson masses equal to the taste-singlet sea-sea meson masses.

B_K at NLO in the 1+1+1 PQ theory is

$$\left(\frac{B_K}{B_0}\right)^{\mathrm{PQ},1+1+1} = 1 + \frac{1}{16\pi^2 f_{xy}^2 m_{xy}^2}\left[I_{conn} + I_{disc}^{1+1+1}\right] + c_1 a^2 + c_2 m_{xy}^2 + c_3\frac{(m_X^2 - m_Y^2)^2}{m_{xy}^2} + c_4(m_{U_P}^2 + m_{D_P}^2 + m_{S_P}^2)\ . \tag{45}$$

The connected 1-loop contribution, I_{conn}, comes from evaluating the integral in Eq. (38):

$$I_{conn} = 2m_{xy}^4\widetilde{\ell}(m_{xy}^2) - \ell(m_X^2)(m_X^2 + m_{xy}^2) - \ell(m_Y^2)(m_Y^2 + m_{xy}^2), \tag{46}$$

while the disconnected contribution, I_{disc}^{1+1+1}, comes from evaluating the integral in Eq. (39):

$$I_{disc}^{1+1+1} = \frac{1}{3}(m_X^2 - m_Y^2)^2\frac{\partial}{\partial m_X^2}\frac{\partial}{\partial m_Y^2}\left\{\sum_j \ell(m_j^2)\left(m_{xy}^2 + m_j^2\right)R_j^{[4,3]}(\{M_{XY,I}^{[4]}\};\{\mu_I^{[3]}\})\right\}. \tag{47}$$

In the above expressions, ℓ and $\widetilde{\ell}$ are integrals regulated using the standard SχPT scheme [19, 20]:

$$\int \frac{d^4q}{(2\pi)^4}\frac{1}{q^2+m^2} \to \frac{1}{16\pi^2}\ell(m^2), \tag{48}$$

$$\int \frac{d^4q}{(2\pi)^4}\frac{1}{(q^2+m^2)^2} \to \frac{1}{16\pi^2}\widetilde{\ell}(m^2), \tag{49}$$

One can completely account for lattice finite volume effects by turning the above integrals into sums. This yields an additive correction to the chiral logarithms [43]:

$$\ell(m^2) = m^2\left(\ln\frac{m^2}{\Lambda_\chi^2} + \delta_1^{FV}(m\mathrm{L})\right), \qquad \delta_1^{FV}(m\mathrm{L}) = \frac{4}{m\mathrm{L}}\sum_{\vec{r}\neq 0}\frac{K_1(|\vec{r}|m\mathrm{L})}{|\vec{r}|} \tag{50}$$

$$\widetilde{\ell}(m^2) = -\left(\ln\frac{m^2}{\Lambda_\chi^2} + 1\right) + \delta_3^{FV}(m\mathrm{L}), \qquad \delta_3^{FV}(m\mathrm{L}) = 2\sum_{\vec{r}\neq 0}K_0(|\vec{r}|m\mathrm{L}) \tag{51}$$

where the difference between the finite and infinite volume result is given by $\delta_i^{FV}(m\mathrm{L})$, and K_0 and K_1 are modified Bessel functions of imaginary argument.

Finally, the residues and sets of meson masses that appear in the 1+1+1 disconnected contribution are defined to be:

$$R_j^{[n,k]}(\{m\},\{\mu\}) \equiv \frac{\prod_{a=1}^k(\mu_a^2 - m_j^2)}{\prod_{i\neq j}(m_i^2 - m_j^2)}, \tag{52}$$

$$\{M_{XY,I}^{[4]}\} \equiv \{m_X, m_Y, m_{\pi_I^0}, m_{\eta_I}\},$$

$$\{\mu_I^{[3]}\} \equiv \{m_{U_I}, m_{D_I}, m_{S_I}\}. \tag{53}$$

and the mass eigenstates of the taste singlet flavor neutral PGB's in the 1+1+1 case are[7]

$$m^2_{\pi^0_I,\eta_I} \;=\; \frac{1}{3}\left[m^2_{U_I}+m^2_{D_I}+m^2_{S_I} \pm \sqrt{m^4_{D_I}-(m^2_{U_I}+m^2_{S_I})m^2_{D_I}+m^4_{S_I}+m^4_{U_I}-m^2_{S_I}m^2_{U_I}}\;\right]. \tag{54}$$

The expression in the 2+1 case is somewhat simpler:

$$\begin{aligned}\left(\frac{B_K}{B_0}\right)^{\mathrm{PQ},2+1} \;&=\; 1+\frac{1}{16\pi^2 f^2_{xy} m^2_{xy}}\left[I_{conn}+I^{2+1}_{disc}\right]+c_1a^2+c_2m^2_{xy}\\ &\quad +c_3\frac{(m^2_X-m^2_Y)^2}{m^2_{xy}}+c_4(2m^2_{D_P}+m^2_{S_P})\;,\end{aligned} \tag{55}$$

where the connected term is the same as in the 1+1+1 case and the disconnected term is

$$I^{2+1}_{disc}=\frac{1}{3}(m^2_X-m^2_Y)^2\frac{\partial}{\partial m^2_X}\frac{\partial}{\partial m^2_Y}\left\{\sum_j \ell(m^2_j)\left(m^2_{xy}+m^2_j\right)R^{[3,2]}_j(\{M^{[3]}_{XY,I}\};\{\mu^{[2]}_I\})\right\}, \tag{56}$$

$$\begin{aligned}\{M^{[3]}_{XY,I}\} &\equiv \{m_X,m_Y,m_{\eta_I}\},\\ \{\mu^{[2]}_I\} &\equiv \{m_{D_I},m_{S_I}\}.\end{aligned} \tag{57}$$

When the up and down quark masses are degenerate, the flavor-neutral, taste-singlet mass eigenstates are:

$$\begin{aligned}m^2_{\pi^0_I} \;&=\; m^2_{U_I}=m^2_{D_I},\\ m^2_{\eta_I} \;&=\; \frac{m^2_{U_I}}{3}+\frac{2m^2_{S_I}}{3}.\end{aligned} \tag{58}$$

The disconnected term also becomes simple enough that we choose to show it explicitly:

$$I^{2+1}_{disc}=\frac{1}{3}\left(I_X+I_Y+I_\eta\right), \tag{59}$$

with

$$\begin{aligned}I_X \;&=\widetilde{\ell}(m^2_X)\frac{(m^2_{xy}+m^2_X)(m^2_{D_I}-m^2_X)(m^2_{S_I}-m^2_X)}{(m^2_{\eta_I}-m^2_X)}\\ &\quad -\ell(m^2_X)\left[\frac{(m^2_{xy}+m^2_X)(m^2_{D_I}-m^2_X)(m^2_{S_I}-m^2_X)}{(m^2_{\eta_I}-m^2_X)^2}+\frac{2(m^2_{xy}+m^2_X)(m^2_{D_I}-m^2_X)(m^2_{S_I}-m^2_X)}{(m^2_Y-m^2_X)(m^2_{\eta_I}-m^2_X)}\right.\\ &\quad \left.+\frac{(m^2_{D_I}-m^2_X)(m^2_{S_I}-m^2_X)-(m^2_{xy}+m^2_X)(m^2_{S_I}-m^2_X)-(m^2_{xy}+m^2_X)(m^2_{D_I}-m^2_X)}{(m^2_{\eta_I}-m^2_X)}\right],\end{aligned} \tag{60}$$

[7] Strictly speaking, in the case where $m_u \neq m_d$, the mass eigenstates of the flavor-neutral sector are not the same as the physical states, π^0_I and η_I. Since the mixing between these two states is negligible (and vanishes in the isospin limit), usually one does not make a distinction between the mass eigenstates and the physical states.

$$I_Y = I_X(X \leftrightarrow Y), \tag{61}$$

$$I_\eta = \ell(m_\eta^2)\frac{(m_X^2 - m_Y^2)^2(m_{xy}^2 + m_{\eta_I}^2)(m_{D_I}^2 - m_{\eta_I}^2)(m_{S_I}^2 - m_{\eta_I}^2)}{(m_X^2 - m_{\eta_I}^2)^2(m_Y^2 - m_{\eta_I}^2)^2}. \tag{62}$$

Note that all of the sea quark dependence appears in the disconnected terms, and that the sum of these terms vanishes for degenerate valence quark masses. It is clear that I_η vanishes when $m_X = m_Y$, but it is not immediately obvious that the other terms go to zero. However, it can be shown that in the limit that $m_X \to m_Y$, $I_X \to -I_Y$ and thus the sum in Eq. (59) vanishes as claimed.

Multiple definitions of the "full QCD" point appear in the mixed action χPT literature. This is because the mixed Ginsparg-Wilson valence, staggered sea theory has no true full QCD point at finite lattice spacing. Thus any choice of how to define the full QCD point should be made for convenience. In this paper, we consider the two cases that most closely resemble the full unquenched theory.

One possible way to define full QCD for the mixed action theory with 2+1 flavors is to set $m_X = m_{D_I} = m_{\pi_I^0}$ and $m_Y = m_{S_I}$. On the lattice, this is nontrivial because it requires a tuning of the bare valence masses in order to set the valence PGB masses to be those of the taste-singlet sea PGB masses. This definition has the advantage, however, that the NLO expression for B_K looks very much like the continuum expression, except for the analytic term proportional to a^2. In this case, the expression for B_K at NLO reduces to

$$\begin{aligned}\left(\frac{B_K}{B_0}\right)^{\text{"full"}} &= 1 + \frac{1}{16\pi^2 f_{xy}^2 m_{xy}^2}\Big[2m_{xy}^4\widetilde{\ell}(m_{xy}^2) + \frac{1}{2}(m_X^2 - 7m_{xy}^2)\ell(m_{\eta_I}^2) - \frac{1}{2}(m_X^2 + m_{xy}^2)\ell(m_X^2)\Big] \\ &+ \widetilde{c}_1 a^2 + c_2 m_{xy}^2 + c_3\frac{(m_X^2 - m_Y^2)^2}{m_{xy}^2} + \widetilde{c}_4(2m_X^2 + m_Y^2),\end{aligned} \tag{63}$$

where we have used the relationship $m_{\eta_I}^2 = (4m_{xy}^2 - m_X^2)/3$ which holds in this limit.[8] This clearly approaches the standard result as $a \to 0$.

A popular, alternative way to define full QCD in MAχPT is to set the valence-valence meson mass equal to the pseudoscalar taste sea-sea meson mass with the same quark content. For perfect G-W valence quarks, this matching condition implies that the renormalized valence quark mass equals the renormalized sea quark mass at tree level in χPT. This is the

[8] Note that the coefficients $\widetilde{c}_1$ and $\widetilde{c}_4$ are different than those in Eqs. (45) and (55) because the mass-squared of the taste-pseudoscalar meson and of the taste-singlet meson differ by a contribution of $\mathcal{O}(a^2)$.

matching condition most often used in mixed action lattice simulations since the Goldstone pion mass vanishes in the chiral limit even at finite lattice spacing. Note that although it is straightforward to set $m_{ij}^{\rm val} = m_{ij}^{\rm sea}$ in the χPT expressions, a lattice calculation using domain wall fermions for the valence quarks would require a non-trivial tuning, since the coefficient which renormalizes the bare domain wall mass is different from that which renormalizes the bare staggered quark mass. The tuning for this case has been done on the MILC lattices by the LHP Collaboration [44], and they find that the renormalization coefficients differ by around 30%. Our formula for B_K to NLO in MAχPT with this choice of tuning (to the taste pseudoscalar) differs from the above tuning to the taste singlet by terms of order a^2. Because no simplification occurs compared to the most general formula, Eq. (45), we do not present a new expression for the tuning to the taste pseudoscalar.

Given that the mixed action theory explicitly violates unitarity at finite lattice spacing, there is no *a priori* reason for preferring one matching condition to another, and there are numerous choices one could make. In the continuum limit, however, all of the matching choices should be identical. At fixed lattice spacing, though, the two choices mentioned above have their advantages and disadvantages. The advantage of matching to the taste singlet is that the theory is described by the full continuum QCD formula (plus an a^2 analytic term), but the disadvantage is that the taste singlet has the largest mass of the 16 taste pions, and on the MILC lattices this mass is still quite large. Matching to the taste pseudoscalar, the lightest of the taste pions, then has the advantage of being closer to the physical pion mass, but it has the disadvantage of having more complicated χPT expressions. However, once the explicit χPT expressions exist, this is not much of a disadvantage. In fact, given the complete partially quenched χPT expressions it is advantageous to not use any tuning at all and to take advantage of additional partially quenched data points in order to best constrain the unknown parameters in the chiral fit. This may not be true for all quantities, especially those for which χPT is not a reasonable guide. In the following numerical analysis we do not assume any matching condition has been chosen; we analyze the results of our more general partially quenched formula.

IV. NUMERICAL ILLUSTRATION OF MIXED ACTION CONTRIBUTIONS TO B_K

We plan on carrying out a mixed action numerical simulation of B_K using domain wall fermions on the publicly available MILC improved staggered ensembles; we therefore use the known parameters and previous measurements on these lattices in order to obtain numerical error estimates for B_K using our χPT results. Currently there are two lattice spacings with large statistics on these ensembles, the "coarse" MILC lattices with $a \approx 0.125$ fm and the "fine" lattices with $a \approx 0.09$ fm. In this section we examine the modifications to the continuum expression for B_K that appear due to finite lattice spacing effects; these include both taste-breaking errors from the staggered sea sector and finite volume errors.

The NLO expression for B_K in a mixed action theory with $2+1$ flavors of sea quarks is given in Eq. (55). Discretization errors lead to two contributions – the shift in the mass-squared of the taste-singlet sea-sea meson that appears in the 1-loop disconnected contribution and the analytic term proportional to a^2. Because we cannot *a priori* know the value of the coefficients of the analytic terms, and because the $\mathcal{O}(a^2)$ analytic term does not arise purely from taste-violating operators, we will neglect analytic terms in this numerical analysis of the size of taste-breaking contributions in B_K. We choose to study discretization errors on the $a \approx 0.125$ fm "coarse" MILC lattices since taste violations will be more pronounced than on the $a \approx 0.09$ fm lattices. In particular, we use the parameters of the ensemble with the lightest up and down sea quark masses on the smaller volume ($L/a = 20$); this ensemble has a light quark mass of $am_l^{\text{sea}} = 0.007$ and a strange quark mass of $am_s^{\text{sea}} = 0.05$.

In order to estimate the size of discretization errors in B_K we calculate the percent difference between the 1-loop contributions to B_K with and without taste-breaking:

$$\eta = \frac{B_K^{1-\text{loop}}(m_l^{\text{val}}, a^2\Delta_I) - B_K^{1-\text{loop}}(m_l^{\text{val}}, 0)}{B_K^{1-\text{loop}}(m_l^{\text{val}}, 0)} \ . \tag{64}$$

In this expression we have set the heavier valence bare quark mass to be equal to the sea strange bare quark mass so that η is a function of the light valence quark mass, m_l^{val}, and the taste-singlet splitting, $a^2\Delta_I$. The taste singlet meson is the heaviest of all of the staggered sea-sea mesons, and $a^2\Delta_I$ is approximately $(450 \text{ MeV})^2$ on the coarse lattices [11]. Because the only sea-sea mesons that contribute to the B_K at 1-loop in the mixed action theory

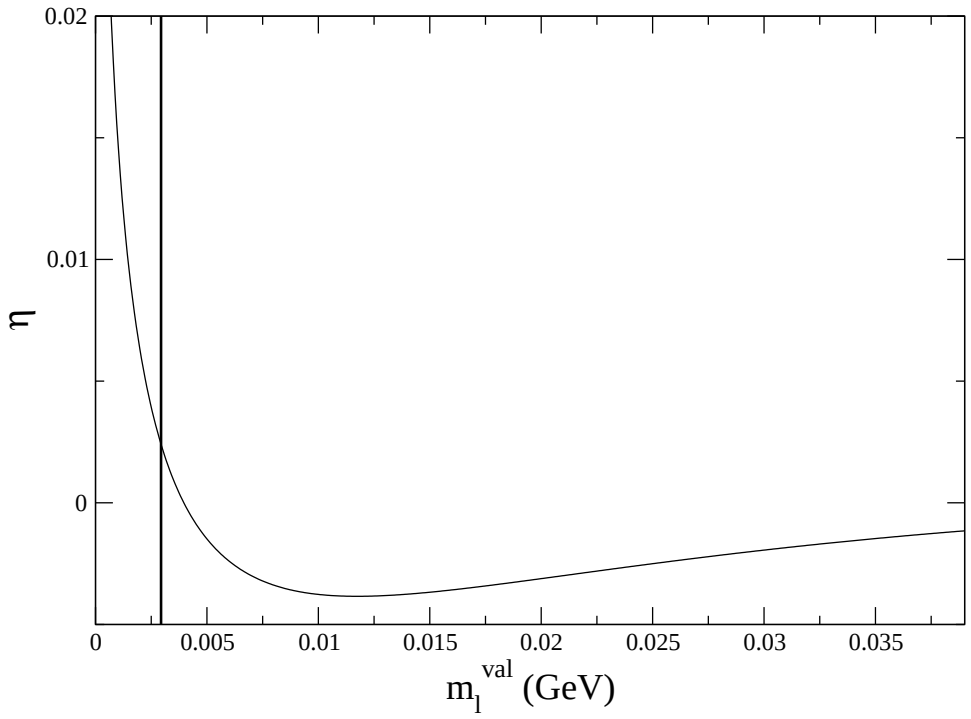

FIG. 3: Percent difference between the 1-loop contributions to B_K with and without taste-breaking discretization errors, Eq. (64), as a function of valence light quark mass. The masses and taste splittings are those of the MILC coarse ensemble ($a = 0.125$ fm) with $am_l = 0.007$ and $am_s = 0.05$. The vertical line shows the physical light quark mass.

are taste-singlets, this large splitting makes the effective sea quark mass considerably larger than a nominal light sea quark mass of $m_s/10$ or $m_s/7$ would suggest. On the fine lattices this splitting is less, close to $(280\text{ MeV})^2$, which scales appropriately according to $a^2\alpha_s^2$ [11], and this shows that it is necessary to approach the continuum limit in order to approach the chiral limit in the sea sector. Note, however, that the sea quark dependence is predicted to be small in the non-analytic contribution to our formulas. The sea quarks only contribute to the disconnected hairpin diagrams in B_K, and this is only around 15% of the connected piece at the physical point. It will, however, be necessary to study the numerical data in order to determine the size of the analytic contribution, as well as to test the validity of our χPT formulas at the physical strange quark mass.

We plot the percent difference, Eq. (64), as a function of valence quark mass in Fig. 3, setting $a^2\Delta_I$ to be the value measured in MILC simulations on the coarse lattices [11]. In this plot, the vertical line shows the location of the physical value of the average up/down

quark mass, $m_l^{\rm phys} \approx m_s/27$. One can see that for larger valence light masses, η rapidly goes to zero. This is to be expected as the difference between the mass-squared of purely valence and purely sea mesons will ultimately be negligible for sufficiently large quark masses. At quark masses below $m_l^{\rm val} \approx 0.01$ GeV, η begins to increase as the valence light mass decreases, such that as $m_l^{\rm val} \to 0$, the percent difference blows up rapidly. Note, however, that this dramatic increase does not happen until below the physical mass, so in the region of interest ($m_l^{\rm val} \geq 0.002$ GeV) the error coming from taste violations is never higher than 0.5%. Note also that this estimate depends upon the value of the cutoff, Λ_χ, used (Fig. 3 uses $\Lambda_\chi = 1$GeV), although any cutoff dependence can be absorbed into the analytic terms which are not included in this numerical analysis. Varying Λ_χ within the range of 0.5 GeV to 1.5 GeV changes this picture in the relevant light quark mass range only by a nearly constant vertical shift at the half a percent level.

As for the analytic terms, if all terms up to NLO were included in Eq. (64) this ratio would be explicitly independent of those analytic terms present in the continuum. The remaining term which is proportional to a^2 has been set to zero since we do not know *a priori* its value. In our analysis, however, by choosing a non-zero value for c_1, our plot in Fig. 3 would just shift vertically by a nearly constant amount as a function of the quark mass in the region of interest. If the scaling dependence of quenched domain wall fermions with various gauge actions is any guide (see Fig. 7 of Ref. [45]), this term will give a contribution that is on the order of a few percent.

We now repeat the above analysis, but include errors due to the finite spatial extent of the lattice. Such finite volume effects can be quite noticeable at the lightest sea quark masses available on the MILC configurations. One might imagine that the finite volume effects in the mixed case would not be very different than the continuum case, since the taste violating effects only enter through the taste singlet meson, which has a large mass. In actuality, this is precisely where there could be a problem, since the heavy singlet mass appears only in the sea sector. Partially quenched pathologies begin to appear when $m_\pi^{\rm val} < m_\pi^{\rm sea}$.[9] Consequently, if the sea mesons are significantly heavier than the valence mesons (as they are in the mixed action theory) these pathologies may become more pronounced. We will see that this is, in fact, the case.

[9] See, for example, Ref. [46].

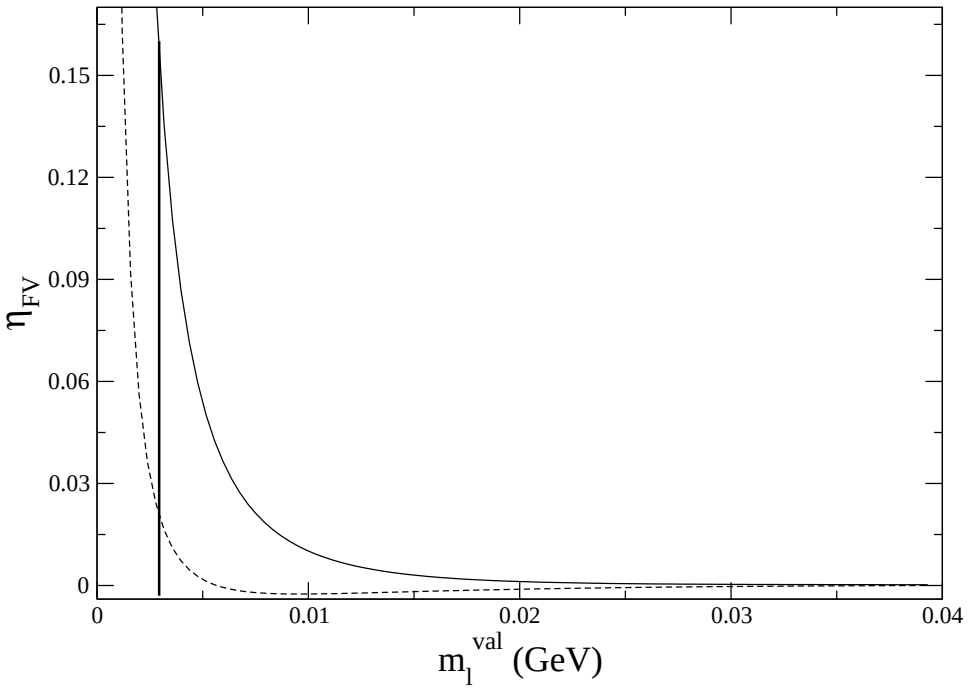

FIG. 4: Percent difference in the 1-loop contributions to B_K in finite and infinite volume, Eq. (65), as a function of valence light quark mass. The dashed curve corresponds to η_{FV} with $a^2\Delta_I = 0$ (the continuum case), and the solid curve shows η_{FV} with $a^2\Delta_I$ set to its value on the coarse ($a = 0.125$ fm) MILC lattices. The sea quark masses are $am_l = 0.007$ and $am_s = 0.05$, and the spatial extent of the lattice is $L = 20$.

In analogy with Eq. (64), we define η_{FV} to be the percent difference between the 1-loop contribution to B_K in the mixed theory at finite volume and B_K in the mixed theory at infinite volume, both including discretization errors:

$$\eta_{FV}(m_l^{\rm val}, a^2\Delta_I) = \frac{B_K^{1-{\rm loop,FV}}(m_l^{\rm val}, a^2\Delta_I, L) - B_K^{1-{\rm loop}}(m_l^{\rm val}, a^2\Delta_I)}{B_K^{1-{\rm loop}}(m_l^{\rm val}, a^2\Delta_I)} \ . \tag{65}$$

We evaluate the above expression at a spatial lattice size of $L = 20$; the remaining parameters are the same as in the previous analysis. We then plot in Fig. 4 two curves – the dashed curve shows the percent difference in Eq. (65) for the continuum limit, $\eta_{FV}(m_l^{\rm val}, 0)$, while the solid curve shows the same percent difference with $a^2\Delta_I$ set to its value on the coarse MILC lattices. Again, the vertical line indicates the physical light quark mass.

One can see that, for the region $m_l^{\rm val} \geq 0.01$ GeV, the error associated with finite volume effects, while not negligible, is quite small, of $\mathcal{O}(1\%)$ or less. Although the continuum and

finite lattice spacing cases are different, in each instance finite volume effects are small. As the valence light quark mass drops below the sea light quark mass, the error shoots up rapidly, which is expected because quenching artifacts (where finite volume effects are more pronounced) become more noticeable in this region. As discussed above, the mixed case sees these quenching artifacts at a larger valence mass, since the sea mesons are heavier. Although one might worry about this significant difference between the continuum and the mixed cases for the lighter masses (the difference is rather striking at the physical mass), this is not a practical problem. For example, the MILC ensemble with a light sea quark mass of $am_l^{\rm sea} = 0.005$ has a spatial length of $L = 24$ as opposed to 20 for the heavier sea quark mass ensembles. This increase in volume for the lighter quark mass was chosen by MILC to reduce finite volume effects for such a light sea quark mass [2]. In our planned simulations of B_K, the quantity which we wish to keep large is the combination $m_\pi^{val} L$, which as a general rule-of-thumb should be 4 or more to keep the finite volume effects relatively small.[10] Note though, that in Fig. 4, the renormalized valence quark mass $m_l^{\rm val} = 0.01$ GeV, and with L=20 this corresponds to an $m_\pi L \approx 3$, leading to a finite volume relative error of about 1.5%. As the valence quark mass (and thus the valence pion mass) decreases, this error goes up rapidly. If we want to go to lighter quark masses, we will need to use the MILC lattices with larger volume (L=24) so that $m_\pi^{val} L$ does not become significantly smaller than 3, and the finite volume corrections stay below the 2% level. The key point is that simulations are done to the right of this "wall" in Fig. 4 at which the error explodes, so one can correct for finite volume errors before performing extrapolations to the continuum and physical light quark mass.

V. CONCLUSIONS

In this work we have calculated the expression for B_K in a mixed action lattice theory with Ginsparg-Wilson valence quarks and staggered sea quarks to next-to-leading order in chiral perturbation theory. We have discussed in some detail how to extend the continuum

[10] Although finite volume χPT at can be used to correctly describe more significant finite size errors, if the removable 1-loop finite volume corrections to B_K are around 15%, then it is likely that the remaining 2-loop finite volume errors will still be a few percent. Such a large systematic uncertainty from finite size effects is unacceptable if one is aiming for an overall error of 5% in B_K.

calculation to the mixed action case, and we have provided expressions for both a "1+1+1" partially quenched theory ($m_u \neq m_d \neq m_s$) and a "2+1" partially quenched theory ($m_u = m_d \neq m_s$), both of which reduce to the corresponding partially quenched QCD expressions in the continuum limit.

It is illustrative to compare our expression for B_K in mixed action chiral perturbation theory to that for other lattice theories. Four parameters are needed to describe B_K in the continuum: one leading order constant, B_0, and three NLO coefficients. In the case of pure Ginsparg-Wilson lattice fermions, the expression for B_K contains one additional coefficient proportional to a^2. For domain-wall lattice fermions there is an additional constant, $m_{\rm res}$, which comes from chiral symmetry breaking due to the finite domain wall separation. This term simply enters B_K as an additive shift to the quark mass and can be separately measured in a tree-level fit to the pion mass-squared. In the mixed action lattice theory with staggered sea quarks and domain wall valence quarks that we have considered here, taste-symmetry breaking effects produce an additive shift to the sea-sea meson mass squared. This is the only new term that appears in the calculation of B_K with domain-wall quarks on a staggered sea as compared to a pure domain-wall calculation. In contrast, the expression for B_K with staggered valence quarks on a staggered sea contains many new parameters, each of which must be determined from lattice simulations and subsequently removed in order to extract the value of B_K in the continuum. It is interesting to note that the expression for B_K in the mixed G-W, staggered lattice theory is no more complicated than that for a domain-wall simulation in which a different value of the domain-wall separation is used in the valence and sea sectors; such a "mixed" domain-wall simulation was previously proposed in Ref. [47]. In this case the value of $m_{\rm res}$ would differ in the valence and sea sectors, and the corresponding expression for B_K could be gotten from our expression, Eq. (45), by simply making the replacements $m_{\rm res} \to m_{\rm res}^{\rm valence}$ and $a^2\Delta_I \to m_{\rm res}^{\rm sea}$. Thus the taste-singlet sea-sea meson mass shift can be thought of as an effective $m_{\rm res}$ in the sea sector, though this effective "$m_{\rm res}$" scales as a^2, and consequently vanishes in the continuum limit.

Finally, we have presented a numerical analysis of the resulting expressions in which we have examined the size of discretization errors from taste-symmetry breaking in the sea sector and finite volume errors for the MILC coarse ($a \approx 0.125$ fm, L=20 and 24) lattice ensembles. We find that the non-analytic taste-breaking contributions to B_K in the mixed action theory are around 0.5% over the range of the extrapolation and so are quite small. The

finite volume effects are somewhat larger for the mixed action case than in the continuum, but still remain at or below the 2%- level for the values of the light quark masses used to generate the MILC ensembles. It will of course be necessary to study the numerical lattice data in order to determine the size of the analytic contribution, as well as to test the validity of our NLO χPT formulas at the physical strange quark mass.

A lattice calculation of B_K using domain-wall valence quarks on top of improved staggered field configurations combines the best properties of both fermion discretizations. This method will be competitive with other established methods for calculating B_K, and ultimately it should give a useful constraint on the CKM matrix and phenomenology.

Acknowledgments

We thank Andreas Kronfeld, Donal O'Connell and André Walker-Loud for useful discussions and careful readings of the manuscript. We are grateful to Steve Sharpe and Claude Bernard for useful comments. We also thank the Institute for Nuclear Theory at the University of Washington for their hospitality while some of this work was completed. CA would like to thank Norman Christ for useful discussions. This research was supported by the DOE under grant nos. DE-FG02-92ER40699 and DE-AC02-76CH03000.

---

[1] C. T. H. Davies et al. (HPQCD), Phys. Rev. Lett. **92**, 022001 (2004), hep-lat/0304004.

[2] C. Aubin et al. (MILC), Phys. Rev. **D70**, 114501 (2004), hep-lat/0407028.

[3] I. F. Allison et al. (HPQCD), Phys. Rev. Lett. **94**, 172001 (2005), hep-lat/0411027.

[4] E. Gamiz et al. (HPQCD) (2006), hep-lat/0603023.

[5] J. Kim, T. Bae, and W. Lee, PoS **LAT2005**, 338 (2005), hep-lat/0510007.

[6] S. D. Cohen, PoS **LAT2005**, 346 (2005), hep-lat/0602020.

[7] M. Bona et al. (UTfit Collaboration), URL `http://utfit.roma1.infn.it/`.

[8] J. Charles et al. (CKMfitter Group), URL `http://ckmfitter.in2p3.fr/`.

[9] S. Eidelman et al. (Particle Data Group), Phys. Lett. **B592**, 1 (2004).

[10] C. W. Bernard et al., Phys. Rev. **D64**, 054506 (2001), hep-lat/0104002.

[11] C. Aubin et al., Phys. Rev. **D70**, 094505 (2004), hep-lat/0402030.

[12] C. Bernard, Phys. Rev. **D73**, 114503 (2006), hep-lat/0603011.

[13] M. Creutz (2006), hep-lat/0603020.

[14] C. Bernard, M. Golterman, Y. Shamir, and S. R. Sharpe (2006), hep-lat/0603027.

[15] C. Bernard, M. Golterman, and Y. Shamir (2006), hep-lat/0604017.

[16] Y. Shamir (2006), hep-lat/0607007.

[17] S. R. Sharpe, PoS. **LAT2006**, 022 (2006), hep-lat/0610094.

[18] W.-J. Lee and S. R. Sharpe, Phys. Rev. **D60**, 114503 (1999), hep-lat/9905023.

[19] C. Aubin and C. Bernard, Phys. Rev. **D68**, 034014 (2003), hep-lat/0304014.

[20] C. Aubin and C. Bernard, Phys. Rev. **D68**, 074011 (2003), hep-lat/0306026.

[21] S. R. Sharpe and R. S. Van de Water, Phys. Rev. **D71**, 114505 (2005), hep-lat/0409018.

[22] C. Aubin and C. Bernard, Phys. Rev. **D73**, 014515 (2006), hep-lat/0510088.

[23] D. Verstegen, Nucl. Phys. **B249**, 685 (1985).

[24] G. Martinelli, C. Pittori, C. T. Sachrajda, M. Testa, and A. Vladikas, Nucl. Phys. **B445**, 81 (1995), hep-lat/9411010.

[25] R. S. Van de Water and S. R. Sharpe (2005), hep-lat/0507012.

[26] W.-j. Lee and S. R. Sharpe, Phys. Rev. **D68**, 054510 (2003), hep-lat/0306016.

[27] T. Becher, E. Gamiz, and K. Melnikov, Phys. Rev. **D72**, 074506 (2005), hep-lat/0507033.

[28] P. H. Ginsparg and K. G. Wilson, Phys. Rev. **D25**, 2649 (1982).

[29] D. B. Kaplan, Phys. Lett. **B288**, 342 (1992), hep-lat/9206013.

[30] Y. Shamir, Nucl. Phys. **B406**, 90 (1993), hep-lat/9303005.

[31] R. Narayanan and H. Neuberger, Phys. Lett. **B302**, 62 (1993), hep-lat/9212019.

[32] R. Narayanan and H. Neuberger, Nucl. Phys. **B412**, 574 (1994), hep-lat/9307006.

[33] R. Narayanan and H. Neuberger, Nucl. Phys. **B443**, 305 (1995), hep-th/9411108.

[34] B. Bistrovic et al. (Lattice Hadron Physics), J. Phys. Conf. Ser. **16**, 150 (2005).

[35] S. R. Beane, P. F. Bedaque, K. Orginos, and M. J. Savage (NPLQCD), Phys. Rev. **D73**, 054503 (2006), hep-lat/0506013.

[36] O. Bär, C. Bernard, G. Rupak, and N. Shoresh, Phys. Rev. **D72**, 054502 (2005), hep-lat/0503009.

[37] J. Bijnens, H. Sonoda, and M. B. Wise, Phys. Rev. Lett. **53**, 2367 (1984).

[38] T. Blum et al., Phys. Rev. **D66**, 014504 (2002), hep-lat/0102005.

[39] T. Blum et al. (RBC), Phys. Rev. **D68**, 114506 (2003), hep-lat/0110075.

[40] Y. Aoki et al., Phys. Rev. **D73**, 094507 (2006), hep-lat/0508011.

[41] J.-W. Chen, D. O'Connell, R. S. Van de Water, and A. Walker-Loud, Phys. Rev. **D73**, 074510 (2006), hep-lat/0510024.

[42] C. Bernard, T. Draper, A. Soni, H. D. Politzer, and M. B. Wise, Phys. Rev. **D32**, 2343 (1985).

[43] C. Bernard (MILC), Phys. Rev. **D65**, 054031 (2002), hep-lat/0111051.

[44] D. B. Renner et al. (LHP), Nucl. Phys. Proc. Suppl. **140**, 255 (2005), hep-lat/0409130.

[45] W. Lee (2006), hep-lat/0610058.

[46] C. W. Bernard and M. F. L. Golterman, Phys. Rev. **D49**, 486 (1994), hep-lat/9306005.

[47] M. Golterman and Y. Shamir, Phys. Rev. **D71**, 034502 (2005), hep-lat/0411007.